Structures and Vibrational Spectra of the Sulfur-Rich Oxides SnO (n = 4–9): The Importance of π*–π* Interactions

ARTICLE *in* CHEMISTRY · JANUARY 2007

Impact Factor: 5.73 · DOI: 10.1002/chem.200600393 · Source: PubMed

3 AUTHORS, INCLUDING:

Yana Steudel
John Wiley And Sons
38 PUBLICATIONS **300** CITATIONS
SEE PROFILE

Ralf Steudel
Technische Universität Berlin
357 PUBLICATIONS **4,579** CITATIONS
SEE PROFILE

CHEMISTRY
A EUROPEAN JOURNAL

DOI: 10.1002/chem.200600393

Structures and Vibrational Spectra of the Sulfur-Rich Oxides S_nO (n = 4–9): The Importance of π*–π* Interactions

Ming Wah Wong,*[a] Yana Steudel,[b] and Ralf Steudel*[b]

Abstract: The structures of a large number of isomers of the sulfur oxides S_nO with n = 4–9 have been calculated at the G3X(MP2) level of theory. In most cases, homocyclic molecules with exocyclic oxygen atoms in an axial position are the global minimum structures. Perfect agreement is obtained with experimentally determined structures of S_7O and S_8O. The most stable S_4O isomer as well as some less stable isomers of S_5O and S_6O are characterized by a strong π*–π* interaction between S=O and S=S groups, which results in relatively long S–S bonds with internuclear distances of 244–262 pm. Heterocyclic isomers are less stable than the global minimum structures, and this energy difference approximately increases with the ring size: 17 (S_4O), 40 (S_5O), 32 (S_6O), 28 (S_7O), 45 (S_8O), and 54 kJ mol^{-1} (S_9O). Owing to a favorable π*–π* interaction, preference for an axial (or *endo*) conformation is calculated for the global energy minima of S_7O, S_8O, and S_9O. Vapor-phase decomposition of S_nO molecules to SO_2 and S_8 is strongly exothermic, whereas the formation of S_2O and S_8 is exothermic if $n<7$, but slightly endothermic for S_7O, S_8O, and S_9O. The calculated vibrational spectra of the most stable isomers of S_6O, S_7O, and S_8O are in excellent agreement with the observed data.

Keywords: ab initio calculations · isomers · molecular structures · sulfur oxides · vibrational spectra

Introduction

Sulfur is one of the most oxophilic elements that forms numerous binary oxides.[1,2] Up to now, the following 16 molecular species of type S_nO_m (m = 1–4; n = 1–12) have been detected experimentally: SO, SO_2, SO_3, SO_4, S_2O, S_2O_2, S_2O_3, S_3O, S_5O, S_6O, S_7O, S_7O_2, S_8O, S_9O, $S_{10}O$, and $S_{12}O_2$.

Furthermore, polymeric sulfur oxides, such as α-SO_3 and β-SO_3, as well as peroxides $(SO_{3+x})_n$ with $0<x<1$ and additional polymeric suboxides of composition S_xO ($x>2$), have been prepared.[1] No other element has so many binary oxides. Needless to say that some of these species play an important role in the large-scale production of sulfuric acid, in combustion processes of sulfur-containing fuels, and consequently also in environmental chemistry, just to name a few.

The largest group within the multitude mentioned above are the so-called "lower sulfur oxides" with an oxidation number of the S atom(s) of less than +4. Most of these compounds can be formally derived from the corresponding sulfur molecules S_n (n = 1–12) by adding one or two oxygen atoms to single sulfur atoms. In fact, oxidation of the homocycles S_6, S_7, S_8, S_9, and S_{10} by trifluoroperoxyacetic acid in methylene chloride solution (Reaction (1)) has provided many of the mentioned species.[3]

$$S_n + CF_3CO_3H \rightarrow S_nO + CF_3CO_2H \quad (1)$$

The crystalline compounds S_6O (2 allotropes),[4] S_7O,[5] S_7O_2,[6] S_8O,[7] S_9O,[8] and $S_{10}O$[8] have been prepared in this way. However, X-ray structural analyses are only available for S_7O[9,10] and S_8O.[11] These analyses revealed that the

[a] Prof. Dr. M. W. Wong
Department of Chemistry, National University of Singapore
3 Science Drive 3, Singapore 117543
Fax: (+65) 677-91-691
E-mail: chmwmw@nus.edu.sg

[b] Dr. Y. Steudel, Prof. Dr. R. Steudel
Institut für Chemie, Technische Universität Berlin, Sekr. C2
10623 Berlin (Germany)
Fax: (+49) 30-3142-6519
E-mail: steudel@sulfur-research.de

Supporting information for this article is available on the WWW under http://www.chemeurj.org/ or from the author. This information includes total energies and atomic coordinates of all optimized structures [(B3LYP/6-31G(2df)] shown in Figures 1, 4, 5, and 6; selected bond angles and torsion angles; vibrational frequencies of the heterocyclic S_nO isomers; optimized geometries of **1a** and **1b** at various levels of theory.

oxygen atoms are exocyclic and are present as sulfoxide groups. The homocycles in these oxides exhibit the same conformation as in the corresponding pure sulfur allotropes. In all other cases, however, only spectroscopic data are available to support the anticipated homocyclic molecular structures of these oxides. Therefore, we have undertaken a systematic study of the structures and vibrational spectra of the species S_nO ($n>3$) by means of ab initio MO and density functional calculations.

Previous calculations using density functional theory (DFT) have demonstrated that various homocyclic and heterocyclic structures of S_7O[12] and S_7O_2[13] correspond to minima on the potential energy hypersurfaces (PES), and, in the case of S_7O, the experimental structure was confirmed as the global minimum. Similarly, ab initio calculations of S_3O[14] and S_5O[15] established the homocyclic structures as global (S_3O) or local (S_5O) minima. However, in the present work, we were particularly interested in the question whether the more sulfur-rich monoxides S_4O to S_9O can also exist as heterocycles or, for the smaller molecules, as open-chain isomers on the particular PES, in addition to the expected homocyclic structures.

These oxidized sulfur-rich species as well as related compounds containing the structural unit -S–S(=O)-S- are often said to contain a "branched sulfur chain". It has been shown before that such compounds are likely intermediates[16] in the industrial Claus process,[17] which is used to convert hydrogen sulfide on a large scale to elemental sulfur via the combustion and comproportionation reactions given in Equation (2) and (3).

$$H_2S + {}^3/_2\,O_2 \rightarrow SO_2 + H_2O \quad (2)$$

$$2\,H_2S + SO_2 \rightarrow {}^3/_8\,S_8 + 2\,H_2O \quad (3)$$

In this way, the huge amounts of H_2S obtained from the "sweetening" process of "sour" natural gas[18] as well as from crude oil desulfurization by the HDS process (hydrodesulfurization)[19] are detoxified and turned into a useful raw material for the production of sulfuric acid and other sulfur-containing chemicals as well as for rubber vulcanization.

Computational Details

The structures and energies of various isomeric structures of S_nO were examined at the G3X(MP2) level of theory.[20] This composite method corresponds effectively to QCISD(T)/G3XL//B3LYP/6-31G(2df,p) energy calculations together with zero-point vibrational and isogyric corrections. G3X(MP2) theory represents a modification of the G3(MP2)[21] theory with three important changes: 1) B3LYP/6-31G(2df,p) geometry, 2) B3LYP/6-31G(2df,p) zero-point energy, and 3) addition of a *g* polarization function to the G3Large basis set for the second-row atoms at the Hartree–Fock level. All three features are particularly important for the proper description of the sulfur-containing species examined in this publication. Harmonic fundamental vibrations were calculated at the B3LYP/6-31G(2df,p) level to characterize stationary points as equilibrium structures, with all frequencies real, and transition states, with one imaginary frequency. For selected S_4O isomers, the structures and energies were also examined at the MP2, MP3, MP4, CCSD, and CCSD(T) levels of theory using a variety of basis sets, including cc-pVTZ and aug-cc-pVTZ. Multiconfiguration SCF calculations, including CASSCF,[22] second- and third-order multireference perturbation (CASPT2 and CASPT3),[23] and multireference configuration interaction (MRCI),[24] were carried out for the isomeric structures of S_4O. RHF was used for closed-shell species and the UHF formalism was employed for open-shell systems. For all investigated species, a charge density analysis was performed by using the natural bond orbital (NBO) approach based on the B3LYP/6-31G(2df,p) wavefunction.[25] NBO atomic charges of small molecules have recently been demonstrated to agree well with experimental values obtained from X-ray diffraction data.[26] The topological analysis was carried out with Bader's theory of atoms in molecules (AIM)[27] based on the B3LYP/6-31G(2df,p) wavefunction. Unless otherwise noted, relative energies reported in the text correspond to the G3X(MP2) E_0 values, while all reported structural parameters correspond to the B3LYP/6-31G(2df,p) level. Ab initio and CASSCF calculations were performed with the GAUSSIAN 98[28] and MOLPRO 2002[29] programs, respectively.

Results and Discussion

In the following, the molecular structures of the sulfur-rich oxides will be discussed in the order of increasing sulfur content, beginning with the unknown S_4O, followed by the unstable S_5O, which has only been prepared in solution,[30] and then by the series of homocyclic oxides S_6O to S_9O, which all have been prepared as crystalline solids.[1]

Molecular structures:

S_4O: To the best of our knowledge, this is the first theoretical study on tetrasulfur oxide, which is the only unknown species in the series of S_nO molecules (n = 1–10). Ten local energy minima (**1a**–**f**, **1h**–**k**) have been located on the singlet PES of S_4O, including four cyclic species, four open chains, which all are of SSSSO connectivity, and two branched chains (**1i**, **1k**). In addition, the lowest-energy chainlike triplet isomer (**1g**) is also reported. The geometries and bond lengths of the nine more stable isomers are given in Figure 1; the bond angles and torsion angles are listed in Table S1 in the Supporting Information. The calculated relative energies, enthalpies, Gibbs energies, and dipole moments are summarized in Table 1.

The most stable S_4O isomer (**1a**) is a cyclic molecule with exocyclic S=O and S=S bonds. Interestingly, these two bonds are essentially in one plane (τ(O-S1-S3-S4) = 1.1°). Structure **1a** is characterized by a fairly long central S1–S3 bond of 243.0 pm, which is about 13% larger than the other two S–S distances. Accordingly, the S1–S3 stretching vibration is characterized by a rather low wavenumber of 223 cm^{-1}. The corresponding *trans* conformation (**1b**) is less stable by 13.2 $kJ\,mol^{-1}$. This species has a nonplanar geometry with torsion angles of 109.5° (O-S1-S2-S3), 156.1° (O-S1-S3-S4), and 105.7° (S1-S2-S3-S4). Structures **1a** and **1b** are analogous to the two most stable isomers of the isoelectronic species S_3O_2,[31] which also forms a three-membered homocyclic ring with one S–S bond considerably longer than the other two. However, in the case of S_3O_2, the *trans* conformation is the global minimum.

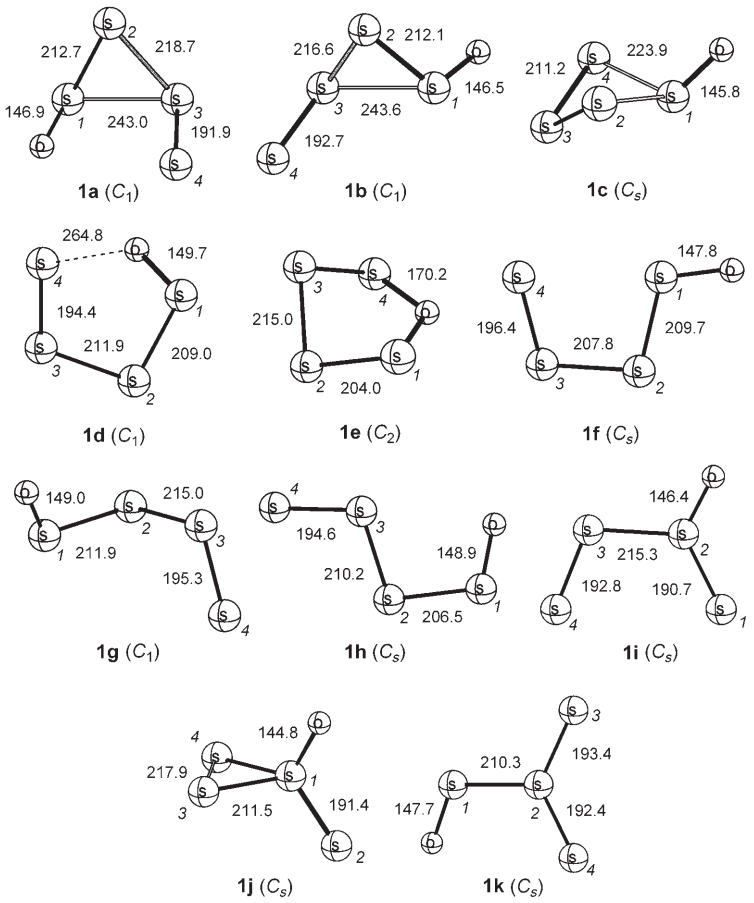

Figure 1. Optimized [B3LYP/6-31G(2df)] geometries of the nine most stable isomers of composition S_4O (bond lengths in pm, symmetries in parenthesis). Species **1g** is a triplet molecule, while all others are singlet species.

Table 1. Calculated relative energies (ΔE_o, ΔH°_{298}, and ΔG°_{298}, kJ mol^{-1})[a] and dipole moments μ[b] [Debye] of eleven isomeric structures of S_4O.

Species	Symmetry	ΔE_o	ΔH°_{298}	ΔG°_{298}	μ
cis-doubly-branched three-membered ring **1a**	C_1	0.0	0.0	0.0	2.45
trans-doubly-branched three-membered ring **1b**	C_1	13.2	13.5	11.9	0.57
branched four-membered ring **1c**	C_s	23.3	23.0	24.1	1.22
cis,*cis*-chain **1d**	C_1	27.3	27.4	27.0	1.99
five-membered ring **1e**	C_1	29.8	29.4	28.6	0.75
cis,*trans*-chain **1f**	C_s	44.2	44.8	42.3	1.34
triplet chain **1g**	C_1	48.4	50.4	38.0	1.03
trans,*cis*-chain **1h**	C_s	53.4	54.5	49.7	2.50
branched chain **1i**	C_s	89.7	88.7	88.7	0.10
doubly-branched three-membered ring **1j**	C_s	109.2	107.9	111.1	1.79
branched chain **1k**	C_s	120.3	120.8	111.8	1.31

[a] Calculated at the G3X(MP2) level; the absolute G3X(MP2) E_0 energy of **1a** is −1666.15239 Hartree. [b] Calculated at the B3LYP/6-31G(2df) level.

The unusual geometrical arrangement in **1a** and **1b** is confirmed by higher-level geometry optimizations at the MP2, MP3, QCISD, CCSD, and CCSD(T) levels with a variety of basis sets (Table S3). It is important to note that the inclusion of *f* polarization functions is essential for a reliable description of long S–S bonds in sulfur-containing molecules.[32] The geometry of **1a** is somewhat sensitive to the level of theory employed. In particular, a longer S1···S3 distance is predicted by methods with a higher level of correlation treatment (Table S3). At our best level of theory [CCSD(T)/cc-pVTZ], the S1-S2-S3 bond angle is 71.1° and the S1···S3 distance is 250.1 pm. The predicted rotational constants of **1a** are 3.00405 (*A*), 1.92727 (*B*), and 1.39297 (*C*) GHz. At the CCSD(T)/aug-cc-pVTZ//CCSD(T)/cc-pVTZ level, **1a** is more stable than **1b** and **1c** by 13.1 and 10.1 kJ mol^{-1}, respectively. As with the prism structure of S_6,[33] and the singlet open-chain forms of S_7,[34] the close contact between atoms S1 and S3 in **1a** and **1b** is attributable to a favorable π*–π* interaction between the terminal S=S and S=O units of the molecule. This π*–π* interaction is reflected in the shape of the highest occupied molecular orbital (HOMO) of **1a** (Figure 2).

To further shed light on the nature of the bonding in **1a**, we examined the topological properties of the electron density, based on Bader's theory of atoms in molecules (AIM).[27] First, we note that all bonds in the O-S1-S2-S3-S4 chain in **1a** are characterized by a maximum electron-density path and its associated bond critical point (bcp). The calculated electron density (ρ_b) as well as the Laplacian ($\nabla^2\rho_b$) values at the bcp are consistent with those of typical covalent bonds. For the long S1···S3 π*–π* interaction, the calculated Laplacian of the electron density ($\nabla^2\rho_b$) is positive, in contrast to the negative value calculated for a typical S–S single bond. The Laplacian contour map in Figure 3 further illustrates that there is little buildup of electron density along the S1···S3 internuclear distance of **1a**. In other words, the relatively short S1···S3 distance cannot be interpreted as a regular covalent single bond. The large ellipticity value (ε = 0.848) in this long S···S bond is consistent with the direction of a π*–π* interaction. The existence of a similar π*–π* bond of length 234.7 pm has recently been proven for the

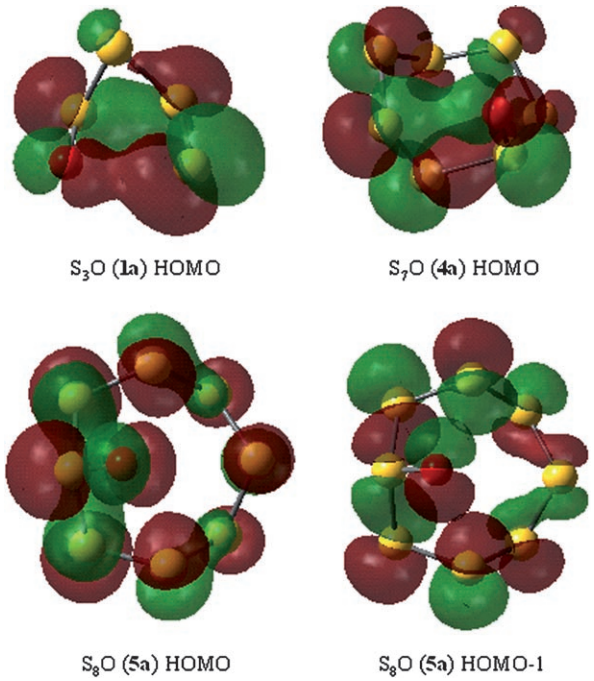

Figure 2. The highest occupied molecular orbitals (HOMO) of tetrasulfur oxide **1a**, of heptasulfur oxide **4a**, and HOMO as well as HOMO-1 of octasulfur oxide **5a**.

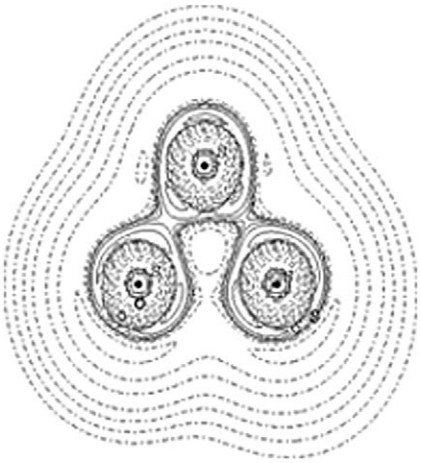

Figure 3. Laplace's contour plot of tetrasulfur oxide **1a** in the plane of the atoms S1, S2, and S3.

isoelectronic S_3O_2 molecule by high-level single- and multireference calculations.[31] S_3O_2 is a 1,2-disulfoxide and has the same conformation as **1b**. In other words, both structures **1a** and **1b** may be considered three-membered rings with one weak S–S bond.

As pointed out in our study of S_3O_2, a diradical resonance form contributes significantly to its electronic structure.[31] Thus, multireference calculations are necessary to provide a proper description of the geometries and energies of **1a** and **1b**. Previous studies have shown that an active space of 2 electrons in 2 orbitals, that is, CAS(2,2), is sufficient to describe the degeneracy problem in S_3O_2[31] and other 1,2-*vicinal*-sulfoxides.[35] Geometry optimizations at the CASPT2/cc-pVTZ level were carried out for **1a**, **1b**, and **1c** with an active space of CAS(2,2). The optimized geometry of **1a** (d(S1–S2) = 210.8, d(S2–S3) = 214.4, d(S1–S3) = 266.8 pm, and α(S1-S2-S3) = 77.7°) is in close agreement with that obtained by single-configuration methods, for example, CCSD(T)/cc-pVTZ. Higher-level MRCI(Q)/aug-cc-pVTZ calculations, based on CASPT2(2,2)/cc-pVTZ geometries, predict that **1a** is more stable than **1b** and **1c** by 3.3 and 1.4 kJ mol^{-1}, respectively. These relative energies are less than those obtained by the single-configuration methods owing to the strong multireference character of **1a**, as reflected in the two dominant configurations (0.823, −0.365). However, the effect of triple excitation is important for a proper description of **1a**. In other words, the relative energies of **1b** and **1c** are likely to be larger. In summary, both single- and multireference calculations indicate that **1a** is the lowest energy structure of S_4O, with a rather interesting geometry.

The most stable truly homocyclic S_4O isomer is the roof-shaped ring **1c** (*cyclo*-tetrasulfur monoxide) with an exocyclic oxygen atom and S-S-S-S torsion angles of ±40.2° and ±37.8°. This structure is less stable by 23.3 kJ mol^{-1} than **1a** and just 6.5 kJ mol^{-1} more stable than the five-membered heterocycle **1e**. In other words, for the composition S_4O, the energy difference between the homocyclic and the heterocyclic isomers (**1c** versus **1e)** is very small and, as we will show below, the smallest among the series of sulfur monoxides S_nO (n = 3–9). However, the screw-shaped (but almost planar) chain **1d** is of intermediate energy with a relative energy of 27.3 kJ mol^{-1}. The small energy differences between **1d** and the cyclic S_4O isomers **1a**, **1b**, **1c**, and **1e** indicate that the ring-opening energies must be quite small.

The two chainlike species **1f** and **1h** lie 44.2 and 53.4 kJ mol^{-1}, respectively, above the global minimum. The structures of these planar zigzag chains are most interesting: the two terminal bonds are very short and correspond to double bonds, whereas the two central S–S bonds of lengths 206.5–210.2 pm may be rationalized as single bonds. The same features can be seen in the structure of the planar S_5O chain **2h** (see below). To a certain extent, these planar isomers may be considered to be derivatives of the S_4 molecule, which also prefers a *cis*-planar chain structure (C_{2v} symmetry).[36] The triplet S_4O chain (**1g**) is a nonplanar molecule with a relative energy of 48.4 kJ mol^{-1}.

In addition, three high-energy isomers of S_4O have been found (relative energies given in parentheses): a branched chain O=S(=S)-S=S (**1i**; 89.7 kJ mol^{-1}), a three-membered homocycle with exocyclic O and S atoms attached to the same ring atom (**1j**; 109.2 kJ mol^{-1}), and another branched chain S=S(=S)-S=O (**1k**; 120.3 kJ mol^{-1}). Isomer **1j** is a derivative of the S_3O molecule, and its ground state is also a homocycle with an exocyclic oxygen atom.[14]

S_5O: The S_5O molecule has been prepared in solution by disproportionation of S_2O followed by dipolar addition of S_2O to the resulting S_3 molecule[15,30] [Eqs. (4) and (5)]:

$$2\,S_2O \rightarrow SO_2 + S_3 \quad (4)$$

$$S_2O + S_3 \rightarrow S_5O \quad (5)$$

Apart from the S–O stretching frequency recorded by IR spectroscopy,[30] no structural information was available for S_5O until a recent study was published on the homocyclic structure of the S_5O molecule (**2a**) calculated at the G3X-(MP2) level; however, other isomers were not considered.[15] Figure 4 shows the seven isomeric structures located on the singlet PES of S_5O as well as the triplet chain **2e**. Bond angles and torsion angles are given in Table S1 in the Supporting Information. The calculated relative energies, enthalpies, Gibbs energies, and dipole moments are presented in Table 2.

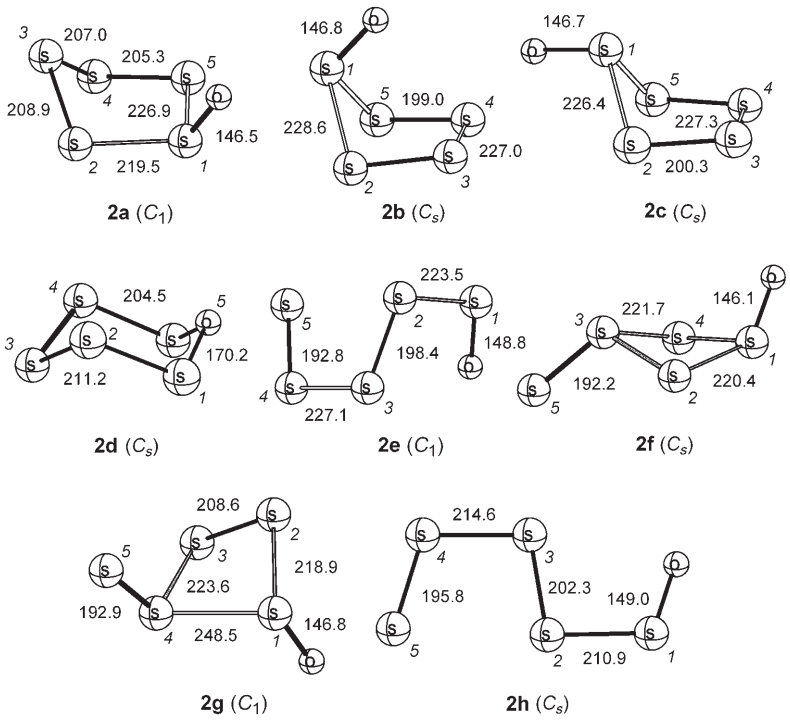

Figure 4. Optimized (B3LYP/6-31G(2df)) geometries of the eight most stable isomers of composition S_5O (bond lengths in pm, symmetries in parenthesis). Except for the triplet chain **2e**, all species are singlet molecules. S–S distances of less than 280 pm are shown as bonds.

The homocyclic S_5O molecule can adopt three different geometries (**2a**–**c**), which all are characterized by a short exocyclic S=O bond of 146.7 ± 0.2 pm and one S-S-S torsion angle close to zero or exactly 0°, resulting in a bond length of 227 pm for the central bond of this structural unit. Such long or "partial" bonds are usually the origin of thermal instability of the corresponding compound. Species **2a** is the most stable isomer, whereas **2b** is 12.9 kJ mol^{-1} less stable. Both isomers have the oxygen atom in an axial position. Structure **2c** with the oxygen atom in an equatorial position is 28.3 kJ mol^{-1} less stable than **2a**. In all three isomers, the S–S bonds adjacent to the sulfoxide group are particularly long (219.5–228.6 pm) and probably highly reactive. This explains why S_5O already reacts with chlorine at −50 °C to thionyl chloride.[30]

Table 2. Calculated relative energies (ΔE_o, ΔH^o_{298}, and ΔG^o_{298}, kJ mol^{-1})[a] and dipole moments μ[b] [Debye] of eight isomeric structures of S_5O.

Species	Symmetry	ΔE_o	ΔH^o_{298}	ΔG^o_{298}	μ
axial branched five-membered ring **2a**	C_1	0.0	0.0	0.0	1.73
axial branched five-membered ring **2b**	C_s	12.9	13.4	12.4	1.61
equatorial branched five-membered ring **2c**	C_s	28.3	29.0	26.9	1.20
six-membered ring heterocycle **2d**	C_s	40.0	38.9	42.4	0.57
triplet chain **2e**	C_1	75.1	77.9	63.1	1.23
1,3-doubly-branched four-membered ring **2f**	C_s	102.4	103.0	100.3	0.86
1,2-doubly-branched four-membered ring **2g**	C_1	104.7	106.0	100.2	0.40
singlet chain **2h**	C_s	123.3	125.6	115.1	0.97

[a] Calculated at the G3X(MP2) level; the absolute G3X(MP2) E_0 energy of **2a** is −2063.93912 Hartree. [b] Calculated at the B3LYP/6-31G(2df) level.

The $[Cp_2MoS_4O]$ complex is an organometallic derivative of isomer **2a** that has been prepared by oxidation of the oxygen-free precursor by *m*-chloroperbenzoic acid at −50 °C via an unstable isomeric species that isomerizes at room temperature to the species shown in Scheme 1 (Cp: η^5-C_5H_5).[37]

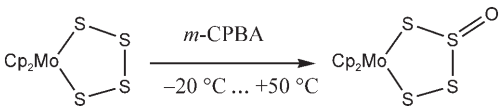

Scheme 1.

According to an X-ray structural analysis, the two S–S bond lengths at the sulfoxide group of $[Cp_2MoS_4O]$ are 207.3 and 210.6 pm, that is, much shorter than the corresponding bonds in **2a**. Evidently, the metal atom has a strong stabilizing (electron-withdrawing) effect.

The six-membered heterocyclic structure **2d** lies 40.0 kJ mol^{-1} and the planar chain **2h** lies 123.3 kJ mol^{-1} above the global minimum of S_5O. However, there are two additional isomers that may both be considered as doubly branched four-membered homocycles (**2f** and **2g**) with an exocyclic oxygen atom as well as one exocyclic sulfur atom. These two species are of very similar energy (102.4 and 104.7 kJ mol^{-1}). The most remarkable feature of **2g** is the

long S–S bond of 248.5 pm. The torsion angle S1-S2-S3-S4 is just 30.4°. As with the global minimum structure of S_4O (**1a**), the long S–S bond in **2g** is attributed to a π*–π* interaction between the terminal S=S and S=O moieties. Hence, **2g** could alternatively be considered as a singlet chain isomer with a *trans*-chain bonding interaction. Isomer **2g** may be an intermediate in the ring-opening reaction of **2a** to give **2h** on the singlet PES. The most stable triplet S_5O isomer, **2e**, is an open-chain species (Figure 4), with marked bond length alternation in the skeleton. Interestingly, there are two planar units in **2e**. This diradical lies 75.1 kJ mol^{-1} above the global minimum (**2a**). Thus, homolytic ring-opening of **2a** requires much more energy than in the case of S_4O (35.2 kJ mol^{-1}), but less energy than in the case of all larger homocyclic sulfur monoxides unless a singlet chain is formed.

S_6O: Two types of crystals of composition S_6O (termed α- and β-S_6O) have been prepared by direct oxygen transfer to *cyclo*-S_6, and both phases have been characterized by Raman spectra,[4] but no other structural information has been available so far. Our calculations show that the homocyclic oxides *exo*-S_6O (**3a**) and *endo*-S_6O (**3b**) with the oxygen atom in either the equatorial or the axial position (Figure 5) differ in energy by just 1.1 kJ mol^{-1}, with the *exo*-conformer slightly favored (both are of C_s symmetry). The chairlike arrangement known from *cyclo*-S_6 is preserved in **3a** and **3b**. Thus, it can be expected that both isomers are formed simultaneously on oxidation of S_6. With an X-ray crystal structure analysis lacking, the comparison of calculated and recorded vibrational spectra may be used to identify these species in the preparative samples (see below). In the presence of $SbCl_5$, S_6O dimerizes to the centrosymmetric homocyclic dioxide $S_{12}O_2$, which has been isolated as an adduct with two molecules of $SbCl_5$ coordinated to the oxygen atoms.[38] This dimerization can now be understood as a dipolar addition reaction in which the S–S(=O) bonds of two molecules combine on account of their high polarity; the atomic charges are +1.04 at the three-coordinate sulfur atom and −0.10 at its neighbors (Scheme 2).

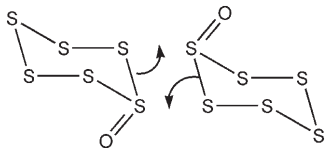

Scheme 2.

An organic derivative of **3a** is the pentathiane-3-oxide $R^1R^2CS_5O$ (R^1 = *t*Bu, R^2 = Ph) containing a twisted CS_5 heterocycle. The connectivity is C-S-S-S(=O)-S-S with S–S bond lengths at the SO group of 215.7 and 218.2 pm,[39] similar to the bond lengths calculated for **3a**.

There is also a seven-membered heterocyclic S_6O isomer of C_1 symmetry (**3c**), which lies 32.1 kJ mol^{-1} above the global minimum structure **3a** (Table 3). This chairlike conformation is analogous to the structure of *cyclo*-S_7, with the smallest S–S–S–S torsion angle of 6.6° (Table S2). Species **3c** exhibits the same S–S bond length alternation around the ring as *cyclo*-S_7,[40] which has previously been explained by through-bond interactions.[41] A formal derivative of **3c** is the organometallic complex $[Cp_2TiOS_5]$ with a seven-membered metallacycle of connectivity Ti-O-S.[42] There are two additional and most unusual isomers of S_6O that may be considered as doubly-branched five-membered homocycles (**3d**,**e**). Their relative energies are 62.6 and 76.2 kJ mol^{-1}, respectively. The oxygen atom and one sulfur atom are exocyclic in these species. Evidently, the structures of **3d** and **3e** are analogous to those of the S_5O isomers **2f** and **2g**. The most stable triplet S_6O isomer is a chain species, characterized by a terminal planar S_4 unit. This diradical species lies 91.5 kJ mol^{-1} above the singlet global minimum (**3a**). Thus,

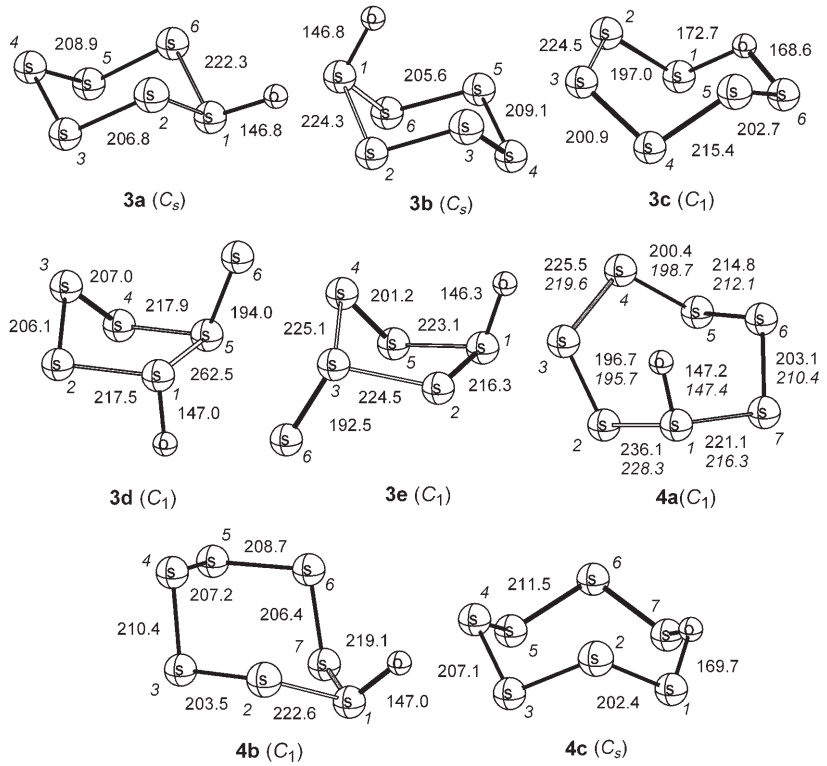

Figure 5. Optimized [B3LYP/6-31G(2df)] geometries and symmetries of five isomers of S_6O (**3a**–**e**) and of three forms of S_7O (**4a**–**c**) with calculated and experimental (in italics) bond lengths (in pm).

Table 3. Calculated relative energies (ΔE_o, ΔH^o_{298}, and ΔG^o_{298}, kJ mol^{-1})[a] and dipole moments μ[b] [Debye] of various isomeric structures of S_6O, S_7O, S_8O and S_9O.

Species		Symmetry	ΔE_o	ΔH^o_{298}	ΔG^o_{298}	μ
S_6O:	**3a**	C_s	0.0	0.0	0.0	1.73
	3b	C_s	1.1	0.9	1.6	1.24
	3c	C_1	32.1	31.5	33.1	0.59
	3d	C_1	62.6	63.8	57.9	1.42
	3e	C_1	76.2	76.8	73.8	0.60
S_7O:	**4a**	C_1	0.0	0.0	0.0	1.32
	4b	C_1	9.2	9.4	6.8	1.71
	4c	C_s	27.6	26.8	28.6	0.46
S_8O:	**5a**	C_s	0.0	0.0	0.0	1.09
	5b	C_s	7.2	7.5	5.9	1.72
	5c	C_1	44.5	44.1	45.3	0.54
S_9O:	**6a**	C_1	0.0	0.0	0.0	0.96
	6b	C_1	0.2	0.6	–0.9	1.85
	6c	C_2	54.0	54.2	51.8	0.32

[a] Calculated at the G3X(MP2) level; the absolute G3X(MP2) E_0 energies of **3a**, **4a**, **5a**, and **6a** are −2461.71013, −2859.4815, −3257.25005, and −3655.01490 Hartree, respectively. [b] Calculated at the B3LYP/6-31G(2df) level.

there is gradual increase in the energy required for homolytic ring opening in this series of sulfur oxides. On the other hand, the ring-opening energy of *cyclo*-S_6 is 146.3 kJ mol^{-1}.[33] Thus, oxidation of S_6 to S_6O results in much more reactive S–S bonds.

S_7O: The global minimum structure of S_7O (**4a**) is homocyclic with the exocyclic oxygen atom in an axial position. This structure exhibits some remarkable features: there are two torsion angles (τ) close to zero (Figure 5). In other words, the molecule has two, almost planar structural units, S2-S3-S4-S5 (τ = −7.6°) and O-S1-S2-S3 (τ = 1.7°), whereas S–S bonds between divalent atoms usually prefer torsion angles close to 90°.[43] As a consequence, the S–S bond lengths of **4a** vary over a wide range from 196.7 to 236.1 pm, which explains the thermal instability of solid S_7O that rapidly decomposes at room temperature.[9] The crystals of heptasulfur oxide contain the molecules in the same conformation as calculated for **4a**.[9,10] Five of the calculated S–S bond lengths agree with the best X-ray data[10] within 2.7 pm (1.3%); however, in two cases, the deviation is much larger, 4.8 and 7.8 pm, with the calculated values larger than the experimental bond lengths. This deviation concerns the two bonds neighboring the SO group. It may well be that the intermolecular SO–SO interaction in solid S_7O[10] is responsible for this deviation, although the experimental SO bond length (147.4 pm) is reproduced within 0.1%. The maximum deviation between calculated and experimental S-S-S-S torsion angles is 2.7°, however, for the O-S1-S2-S3 torsion angle, it is 4.6°, very close to zero.

Another remarkable feature of **4a** is the close contact between the oxygen atom and S3 (301.0 pm), significantly less than the sum of their van der Waals radii (325 pm[44]). Essentially, **4a** exhibits a planar S_3O unit (O-S1-S2-S3), which is characterized by two relatively short S2–S3 and S1–O bonds and two correspondingly long connecting bonds (S1–S2 and S3–O). This feature of a planar four-atom unit is similar to that found in the cluster-like isomer of S_8 that has two three-coordinate atoms.[45] This S_8 cluster isomer is characterized by a rectangular arrangement of four sulfur atoms, with the edges 193 and 281 pm long. This unusual rectangular S_4 rearrangement was rationalized in terms of a π*–π* interaction between the two π* orbitals of the chain-end S=S groups. In the same manner, the planar four-center S_3O arrangement in **4a** is attributed to the attractive interaction between the S=S and S=O moieties, which is evidenced in the HOMO of **4a** shown in Figure 2. This diagram depicts the favorable interaction between the π* orbital of the S1–O unit and the π* orbital of the S2–S3 unit. The importance of the π*–π* interaction is also reflected in the relatively short S2–S3 bond length (196.7 pm), which is of the order of a double bond. In general, two π* orbitals will not give rise to stabilization if both are occupied or both are unoccupied. Stabilization will occur if either both are singly occupied or if one is occupied and the other is unoccupied. In the S_nO species, the π*–π* interaction is probably attributable to the singly occupied π* orbitals. In other words, the diradical resonance structure shown in Scheme 3 is important for the description of the S_nO molecules.

The asymmetrical S_7O isomer **4b** with the oxygen atom also in an axial position, but attached to a different sulfur atom, is 9.2 kJ mol^{-1} less stable than **4a**. This isomer no longer has the two, almost planar four-atom units because the smallest torsion angles S3-S2-S1-S7 (τ = 25.1°) and O-S1-S7-S6 (τ = −48.6°) are now much larger than in the case of **4a**. Considerably less stable, by 27.6 kJ mol^{-1} compared to **4a**, is the heterocyclic isomer **4c**, which has a crown-conformation (Figure 5) similar to S_8 and to the isoelectronic heptasulfur imide S_7NH; the latter is also of C_s symmetry.[46] In contrast to S_7NH, compound **4c** has not yet been prepared. Hohl et al. used molecular dynamics calculations to show how **4c** can be transformed into **4a**.[12]

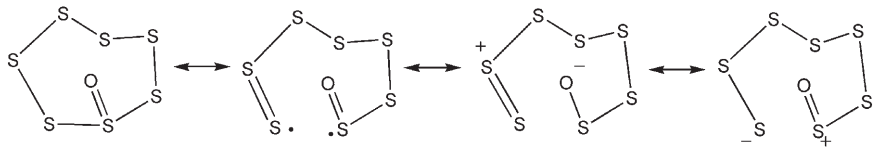

Scheme 3. Resonance structures to describe the bonding in the S_7O molecule **4a**.

S_8O: The structures of three cyclic isomers of composition S_8O are shown in Figure 6; bond angles and torsion angles are listed in Table S2. In agreement with experimental results, the homocyclic derivative with the oxygen atom in an axial position (**5a**) is the most stable form. The conformer with the O atom in an equatorial position (**5b**) is 7.2 kJ mol^{-1} less stable, and the nine-membered heterocycle (**5c**) lies 44.5 kJ mol^{-1} above the energy of **5a**. The total en-

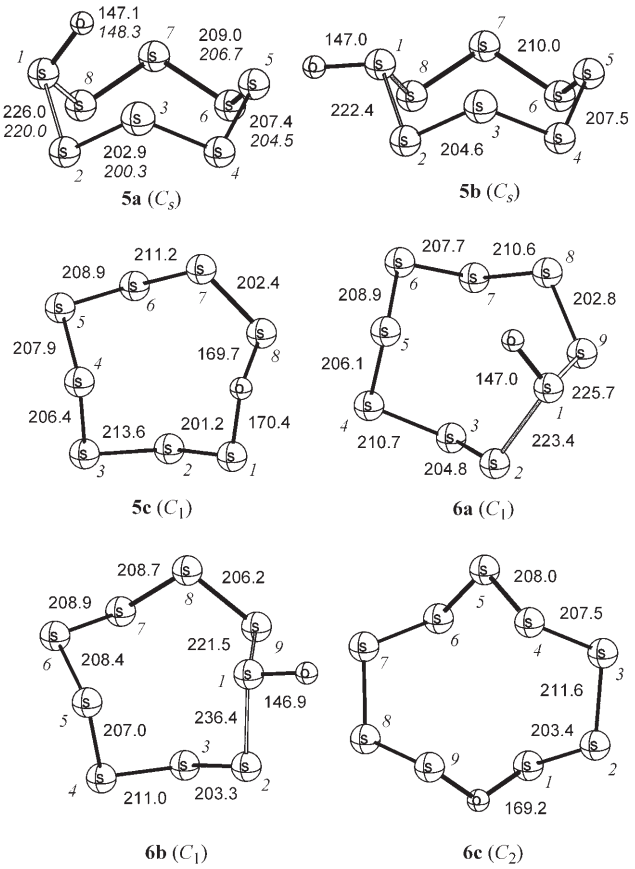

Figure 6. Optimized [B3LYP/6-31G(2df)] geometries and symmetries of the most stable isomers of S_8O (**5a–c**) and S_9O (**6a–c**) with calculated and experimental (in italics) bond lengths (in pm).

ergies as well as relative energies, enthalpies, and Gibbs energies are given in Table 3.

The calculated structure of **5a** is in good agreement with the data from the X-ray structure analysis of single crystals,[11] although the bond lengths are slightly overestimated: calculated S–S bond lengths are up to 6 pm or 3% longer. The data given in Figure 6 are averaged for C_s symmetry. In solid S_8O, there is a strong intermolecular SO···SO interaction, which may influence certain geometrical parameters as well as the SO vibrations. The preference of the axial form (**5a**) over the equatorial conformation (**5b**) can be attributed to π*–π* interactions in **5a**. The exocyclic S=O bond in **5a** forms two planar S_3O units, namely O-S1-S2-S3 and O-S1-S8-S7. The two highest occupied molecular orbitals, HOMO and HOMO-1, of **5a** are depicted in Figure 2. In this case, the π* orbital of the terminal S1–O unit interacts simultaneously with the π* orbital of the S2–S3 and S8–S7 moieties. Note that the two sets of π*–π* interactions in HOMO and HOMO-1 are orthogonal to each other (Figure 2). There is no evidence for an anomeric effect that has previously been postulated to rationalize the preference of the oxygen atom for the axial position as well as to explain the very long S–S bonds adjacent to the S=O group.

The bond-length pattern of isomer **5b** is very similar to that of **5a** and does not deserve any further discussion. It is interesting to note that this isomer is a component of the complex $[S_8O{\cdot}SbCl_5]$ in which S_8O serves as a monodentate ligand connected to the metal atom through the equatorial oxygen atom. On dissolution of this complex in acetone (trapping the $SbCl_5$), the S_8O ligand returns to its most stable conformation, namely **5a**.[47] Interestingly, the heterocyclic isomer of S_8O (**5c**) has the same conformation as the isoelectronic homocycle S_9 with the motif ++−−++−+−.[48,49]

S_9O: This oxide has been prepared by peracid oxidation of *cyclo*-S_9 and has been characterized by Raman spectroscopy. Our calculations show the existence of two homocyclic isomers with almost identical energies on the PES of S_9O (**6a**,**b**). In addition, there is a ten-membered heterocycle **4c** that is 54.0 kJ mol^{-1} less stable (Figure 6). The global minimum structure at 0 K is an asymmetric ring of *endo*-conformation as far as the oxygen atom is concerned (**6a**). The *exo*-conformer **6b** is 0.2 kJ mol^{-1} less stable than **6a** (Table 3). In both cases, the homocycles have the same conformation as the unoxidized S_9 molecule.[48] The absolute values of the torsion angles of **6a** and **6b** vary between 40.9° and 124.4° with the motif ++−−++−+−.

As with S_7O (**4a**), **6a** exhibits a planar S_3O unit, with τ(O-S1-S9-S8) = 6.2° and d(O···S8) = 313.5 pm. Again, this structural feature can be explained in terms of an attractive π*–π* interaction. The ten-membered heterocyclic isomer **6c** has an interesting conformation that is analogous to that of *cyclo*-S_{10}.[50] The oxygen atom is located on the C_2 axis of the molecule, which is the only symmetry element of this molecule.

General aspects of the molecular structures: There are a number of similarities in the geometrical structures as well as in the charge distribution of the most stable and truly homocyclic isomers of the sulfur oxides under discussion. The S=O bond lengths increase slightly with the ring size from 145.8 pm in S_4O (**1b**) to 147.1 pm in S_8O (**5a**) and 147.0 pm in S_9O (**6a**). In turn, the two S–S bonds adjacent to the S=O group are always the longest in the molecule, with bond lengths ranging from 221.1 to 236.1 pm (both in the S_7O isomer **4a**). The bonds neighboring these long S–S bonds are then relatively short (196.7–211.2 pm). In other words, the well-known phenomenon of bond length alternation[1d,9] around the ring is always observed. Except for S_4O, the homocyclic ring of the most stable monoxides S_nO has the same conformation as in the free S_n molecule. In fact, S_4O is a special case in so far as it is the only polysulfur monoxide with a ground state structure that has more the character of a chain rather than a true homocycle, while all others prefer truly homocyclic geometries with an exocyclic oxygen atom.

In previous sections, we have seen the importance of π*–π* interactions in governing the structures of S_4O (**1a**), S_7O (**4a**), S_8O (**5a**), and S_9O (**6a**). From the HOMO-1 of S_8O, depicted schematically in Figure 2, it can be seen that this interaction is attractive between atoms O and S2/S8 but repulsive between S1 and S2/S8, thus explaining the long S–S

bonds originating from the S=O group. The distinctive feature of a π*–π* interaction is the planar arrangement of an S_3O unit with short S–S and S–O bonds (of the order of a double bond) and relatively long connecting S–S (>220 pm) and S–O bonds. For the homocyclic S_4O, S_5O, and S_6O molecules, it is more difficult to accommodate the π*–π* interaction owing to the steric constraints in these smaller rings.

The NBO atomic charges of the oxygen atoms in the most stable sulfur monoxide isomers vary only in the narrow range of −0.81 to −0.86 (see Table 4). The neighboring tricoordinate sulfur atoms always bear a large positive charge (+0.95 to +1.06), while the charges on all other sulfur atoms are much smaller (−0.21 to +0.22). Thus, the S=O bond is highly polar and, therefore, is sometimes depicted as S^+–O^-. However, we prefer to use the symbol S=O to indicate the short internuclear distance. The dipole moments of the S_nO molecules are largest for the *exo*-isomers. No experimental dipole moments of these compounds are known.

Table 4. Dipole moments μ [Debye] and NBO atomic charges of the more stable isomers of the oxides S_4O to S_9O.[a] For numbering of atoms, see Figures 1, 4–6.

Species	μ	O	S1	S2	S3	S4	S5	S6	S7	S8	S9
S_9O **6a**	0.96	−0.85	1.00	−0.12	0.01	0.01	0.02	0.01	−0.01	0.05	−0.10
S_9O **6b**	1.85	−0.85	1.02	−0.10	0.02	0.00	−0.01	0.00	0.00	0.02	−0.10
S_8O **5a**	1.09	−0.85	1.00	−0.11	0.03	−0.01	0.02	−0.01	0.03	−0.11	–
S_7O **4a**	1.32	−0.84	0.97	−0.09	0.04	−0.01	0.02	0.00	−0.09	–	–
S_6O **3a**	1.73	−0.86	1.04	−0.10	0.00	0.01	0.00	−0.10	–	–	–
S_6O **3b**	1.24	−0.85	1.02	−0.11	0.03	0.00	0.03	−0.11	–	–	–
S_5O **2a**	1.73	−0.85	1.01	−0.12	0.03	0.05	−0.13	–	–	–	–
S_4O **1a**	2.45	−0.81	0.95	−0.15	0.22	−0.21	–	–	–	–	–
S_4O **1c**	1.22	−0.83	1.06	−0.11	0.00	−0.11	–	–	–	–	–

[a] Based on the B3LYP/6-31G(2df) wavefunction.

Thermodynamics: All lower sulfur oxides are known to decompose at 20 °C more or less rapidly to sulfur dioxide and elemental sulfur.[1] In the following, we have compiled the standard reaction enthalpies in kJ mol^{-1} for this disproportionation reaction of the most stable isomers [G3X(MP2) level of theory] as a function of the number of sulfur atoms, assuming *cyclo*-S_8 as the only form of sulfur produced [Eq. (6)]:

$$2\,S_nO(g) \rightarrow SO_2(g) + (2n-1)/8\,S_8(g) \quad (6)$$

n:	2	3	4	5
ΔH°_{298}:	−154.9	−241.0	−271.5	−191.3 kJ mol^{-1}
ΔG°_{298}:	−117.6	−215.3	−254.2	−189.3 kJ mol^{-1}
n:	6	7	8	9
ΔH°_{298}:	−166.4	−144.2	−135.0	−145.1 kJ mol^{-1}
ΔG°_{298}:	−177.0	−166.1	−166.8	−188.7 kJ mol^{-1}

If the sulfur-rich oxides are heated in a vacuum, S_2O is produced rather than SO_2.[1] The corresponding (absolute) enthalpies of S_2O formation according to Equation (7) are, of course, much smaller than for SO_2 formation, even if normalized for the same amount of S_nO:

$$S_nO(g) \rightarrow S_2O(g) + (n-2)/8\,S_8(g) \quad (7)$$

n:	3	4	5	6
ΔH°_{298}:	−43.0	−58.2	−18.2	−5.7 kJ mol^{-1}
ΔG°_{298}:	−48.8	−68.3	−35.9	−29.7 kJ mol^{-1}
n:	7	8	9	
ΔH°_{298}:	+5.4	+10.0	+4.9 kJ mol^{-1}	
ΔG°_{298}:	−24.2	−24.6	−35.5 kJ mol^{-1}	

From these data it is evident that the decomposition of S_7O, S_8O, and S_9O with formation of S_2O is mainly entropy driven. Furthermore, the exceptionally low thermodynamic stability of S_3O and S_4O is clearly reflected in the above data, which is a result of the unusual structures of these molecules. On the other hand, S_8O turns out to be the most stable thermodynamically.

Vibrational spectra: All so-called "lower" sulfur oxides give excellent vibrational spectra because the SO group introduces a large local dipole moment giving rise to intense IR absorptions, while the high polarizability of the bonding and antibonding electrons at the sulfur atoms is responsible for the strong Raman scattering of the S–S bonds. For this reason, the vibrational spectra have always been very useful to the experimentalists who first prepared and characterized these thermally unstable compounds. In the following, we discuss the spectra of the more stable species for which experimental data are available. The fundamental modes of the heterocyclic isomers are given in the Supporting Information and will be discussed only briefly. For all isomers it is observed that the well-known mutual dependence of the S–S stretching wavenumbers on the S–S bond lengths[1d,51] is confirmed by our results. This relationship allows the estimation of the internuclear distances from simple spectroscopic experiments.

Whereas the assignment of the calculated frequencies to the different symmetry species is straightforward, the various modes are often strongly coupled owing to the low molecular symmetries. This holds, in particular, for torsion and bending modes, but in some cases also for the stretching vibrations of the long and weak S–S bonds neighboring the SO group. On the other hand, in the low-frequency region, there is a strong overlap of external (lattice) and internal (torsion) modes of the larger rings which make definite assignments difficult.

Table 5. Calculated and observed vibrational spectra of S_8O (**5a**).[a]

Symmetry	Calcd wavenumber (rel. Raman/IR intensity)	Raman spectrum[b]	IR spectrum[c]	Assignment (this work)
a′	1167 (17/100)	1080 w	1094 m/1085 vs 1133 (in CS_2)	ν(SO)
a′	511 (30/9)	516 m	515 w	ν(SS23/78)[d]
a″	508 (10/3)	512 w		ν(SS23/78)
a′	472 (55/1)	474 s		ν(SS45/56)
a″	457 (2/0)			ν(SS45/56)
a′	424 (14/2)	438 w	440 w	ν(SS34/67)
a″	400 (9/10)	423 w	424 w	δ(SSO)
a′	394 (20/10)	395 m	397 s	δ(SSO) + δ(SSS)
a″	362 (15/25)	379 m	383 s	δ(SSO)
a′	318 (88/9)	340 vs	340 w	ν(SS12/78)
a″	281 (33/8)	300 m–s		ν(SS12/78)
a′	244 (3/2)	250 vw		δ(SSS) + τ
a″	231 (8/1)	235 vw		δ(SSS) + τ
a′	206 (100/2)	219 vs		δ(SSS) + τ
a″	183 (4/3)	197 w		δ(SSS)
a′	181 (14/0)	190 w		δ(SSS)
a′	141 (36/2)	157 vs		δ(SSS)
a″	124 (24/1)	140 s		δ(SSS) + τ
a″	124 (19/1)	140 s		δ(SSS) + τ
a″	62 (10/0)	99/84/67/64 m–s		τ and lattice modes
a′	49 (8/1)	44/34/30 m–s		τ and lattice modes

[a] Wavenumbers in cm^{-1} and calculated relative Raman/IR intensities in parentheses. For numbering of sulfur atoms, see Figure 6. Observed intensities: s (strong), m (medium), w (weak), v (very). Modes: ν stretching, δ bending, τ torsion. [b] Solid sample at 20 °C; laser wavelength 568.2 nm. [c] Solid sample at 25 °C. [d] S–S bonds are defined by the number of the atoms involved.

S_8O: By far the best investigated polysulfur monoxide is S_8O. IR and Raman spectra of S_8O have been recorded[52] and assigned by applying a normal-coordinate analysis.[53] Assuming the molecular symmetry to be C_s, there are 12 fundamental modes of a′ symmetry and 9 of a″ symmetry. All modes are Raman-and IR-active. Table 5 gives the calculated wavenumbers and intensities of the harmonic fundamentals compared to the published Raman and IR spectra of solid and dissolved S_8O. The agreement between theory and experiment is excellent, even without scaling. Only the S–O stretching frequency is calculated by 34 cm^{-1} too high, compared to dissolved S_8O. In solid S_8O, this vibration is affected by intermolecular interactions that lead to a lower wavenumber. This interaction can also be seen from the splitting of ν(S–O) into several components in practically all solid oxides investigated in this work (factor group splitting). A comparison of the experimental spectra with the frequencies calculated for *exo*-S_8O (**5b**) showed that there is not such a good agreement, neither for the solid-state spectrum nor for the solution, indicating that the molecule **5a** retains its conformation in solution.

S_7O: In Table 6, Raman and IR spectra of solid and dissolved S_7O[5] are compared to the spectrum calculated for the most stable isomer **4a**. Given the fact that the Raman spectrum has been recorded with a solid sample while the calculated data apply to a separate molecule, the agreement between the calculated wavenumbers and intensities is very satisfactory. The data also show that the molecular conformation is retained in solution since the solution IR data agree perfectly with the Raman wavenumbers. It is interesting to note that S–S stretching modes contribute to wavenumbers scattered over the large range 265–584 cm^{-1}, in accordance with the wide range of S–S bond lengths calculated for **4a**.

S_6O: The spectra calculated for *exo*- and *endo*-S_6O may be used to decide whether the samples of α- and β-S_6O obtained by peracid oxidation of S_6 contain molecules of different conformation. The data in Table 7 indicate that this is clearly the case, but in the sense that both samples are mixtures of *exo*- and *endo*-S_6O with different concentration ratios. Not only do the two forms give identical solution IR spectra,[4] the Raman spectra of α- and β-S_6O are also very similar, at least above 350 cm^{-1}. Below this limit the Raman lines of both forms can either be assigned to *exo*- or to *endo*-S_6O. For example, in the region 295–350 cm^{-1} there is one fundamental mode for *exo*-S_6O (297 cm^{-1}) and two for the *endo*-isomer

Table 6. Calculated and observed vibrational spectra of S_7O **4a**.[a]

Calcd wavenumber (rel. Raman/ IR intensity)	Raman spectrum[b]	IR spectrum[c]	Assignment[d] (this work)
1167 (19/100)	1113/1102/1098 vw–w	1100 m	ν(SO)
584 (19/16)	575 m	577 w	ν(S2S3)
536 (22/6)	534 w	535 w	ν(S4S5)
516 (24/4)	517 m	514 vw	ν(S6S7)
403 (12/9)	402 w	401 w	δ(SSO)
375 (10/3)	372 w–m	367 w	ν(S5S6)
361 (31/13)	345 m		ν(S5S6) + δ-(SSO)
338 (70/2)	325 vs		ν(S3S4)
307 (100/4)	292 s		δ(SSO) + ν-(S1S2)
281 (34/1)	281 m		δ(SSS)
265 (38/3)	243 vw		ν(S1S2) + τ
221 (75/1)	233 s		δ(SSS)
197 (6/1)	193 m		τ
170 (34/2)	165 s		τ
143 (25/0)	158 m		δ(SSS)
127 (13/0)	129 w–m		δ(SSS)
101 (7/1)	94 w–m		τ
67 (4/1)	88/79/74/42/27/ 24 m–s		τ and lattice modes

[a] Wavenumbers in cm^{-1} and calculated relative Raman/IR intensities in parentheses. For numbering of sulfur atoms, see Figure 5. For symbols and abbreviations, see Table 5. [b] Solid sample at −90 °C; laser wavelength 647.1 nm. [c] In $CHBr_3$ at 25 °C. [d] S–S bonds are defined by the number of the atoms involved (see Figure 5).

Table 7. Calculated and observed vibrational spectra of two phases of solid S_6O.[a]

Symmetry	*exo*-S_6O (**3a**) (rel. Raman/IR intensity)	*endo*-S_6O (**3b**) (rel. Raman/IR intensity)	α-S_6O Raman spectrum[b]	β-S_6O Raman spectrum[c]	IR spectrum[d]
a′	1186 (82/100)	1181 (29/100)	1106[2]/1092 [14]	1102 [12]/1097 [1]	1102 (100) 1130[e]
a′	508 (95/3)	494 (80/1)	499 [55]	499 [51]	506 (5)
a″	491 (2/11)	483 (2/3)	486 [4]	488 [14]	494 (10)
a′	459 (17/1)	451 (20/2)	463 [12]	463 [20]	462 (5)
a″	433 (30/10)	423 (23/13)	445 [19]/440 [20]	441 [27]	438 (20)
a′	429 (23/15)	418 (24/10)	414 [37]	406 [29]	414 (20)
a″	383 (0/6)		370 [19]	371 [11]	365 (20)
a″		348 (6/14)	341 [<20]		
a′		315 (100/8)	329 [100]	320 [100]	320 (5)
a′	297 (10/1)		298 [22]/293 [18]	296 [35]	
a′	–	275 (35/1)	279 [28]	279 [60]	–
a″	–	275 (29/2)			
a′	258 (100/2)	–	236 [47]	236 [23]	
a′	227 (16/1)	225 (33/0)		203 [41]	
a″	217 (34/0)	–	193 [87]	194 [57]	
a″	–				
a′	174 (40/0)	184 (45/0)	182 [49]	175 [24]	
a′	–	162 (22/0)			
a″	165 (19/0)	–	162 [5]/154 [4]	160 [8]	
a″	119 (10/1)	134 (2/0)	131 [10]	120 [4]	
a′	91 (2/1)	80 (10/2)	90/78/71/63/52/29[f]	104/101/91/73/57/51/39[f]	

[a] Wavenumbers in cm^{-1}; calculated relative Raman/IR intensities in parentheses and observed relative Raman peak heights in brackets. Both S_6O phases contain traces of S_6, the Raman lines of which have been omitted for clarity. [b] Sample temperature −100 °C. [c] Sample temperature −80 °C. [d] In $CHBr_3$ solution of either α-S_6O or β-S_6O (25 °C). [e] In CS_2 at 25 °C. [f] Torsional and external (lattice) modes.

Table 8. Calculated vibrational spectra of two isomers of S_9O, and experimental Raman spectrum according to reference [8].[a]

endo-S_9O (**6a**) (rel. Raman/IR intensity)	*exo*-S_9O (**6b**) (rel. Raman/IR intensity)	Raman spectrum[b] (Raman intensity)
1169 (19/100)	1181 (100/100)	1129(7)/1121(24)/1116(5)/1113(5)/1105(8)/1101(2)
513 (21/5)	509 (17/4)	517 (19)
487 (13/4)	500 (24/3)	502 (21)
477 (10/4)	472 (10/0)	462 (21)
451 (81/3)	454 (21/2)	448 (25)
445 (15/1)	447 (61/1)	
	429 (44/11)	425 (32)
417 (12/4)	416 (12/3)	407 (33)
398 (9/8)	390 (25/1)	396 (20)
383 (30/2)	381 (18/14)	372 (28)
352 (16/24)		350 (94)
318 (100/5)		314 (11)
288 (23/1)	288 (19/2)	291 (31)
266 (28/2)	272 (53/0)	248 (28)
241 (17/2)	248 (10/0)	240 (100)
220 (9/1)	226 (15/1)	
	210 (36/0)	211 (28)
198 (27/1)	194 (27/1)	
191 (34/2)	180 (24/1)	176 (12)
155 (31/0)	153 (52/0)	165 (53)
139 (19/0)	145 (12/0)	139 (34)/124 (14)
107 (21/2)	108 (12/1)	119 (13)/111 (33)
102 (16/0)		102 (19)
82 (32/0)	85 (36/0)	93 (7)
75 (21/0)	72 (18/0)	78 (36)
	64 (11/0)	63 (15)
46 (7/0)	52 (9/0)	51(43)/40(41)/31(8)/22(33)

[a] Wavenumbers in cm^{-1}, relative Raman/IR intensities in parentheses. [b] Solid S_9O at −100 C; laser wavelength 647.1 nm.

(348 and 315 cm^{-1}). For α-S_6O, three Raman lines have been measured in this region, at 341, 329, and 295 ± 3 cm^{-1}, matching the calculated modes of *exo- and endo*-S_6O quite well. Thus, α-S_6O is clearly a mixture of both isomers. In the case of β-S_6O the Raman lines at 320 and 296 cm^{-1} match one mode each of *exo*- and *endo*-S_6O, but the spectrum of β-S_6O is much simpler than that of the α form. Therefore, one has to assume that β-S_6O is also a mixture, but with a higher concentration of *endo*-S_6O than in α-S_6O. In summary, it is obvious that the recorded spectra are in agreement with the calculated data, but both samples turned out to be mixtures of two conformers. The modes leading to the weak Raman lines at 370 ± 1 cm^{-1} may be activated in the solid state although the calculated Raman intensity is close to zero.

S_9O: There are 24 fundamental modes expected for S_9O. Inspection of the spectroscopic data of the two homocyclic isomers of S_9O in Table 8 leads to the result that the S_9O sample obtained by peracid oxidation of *cyclo*-S_9 consists of both *endo*- and *exo*-S_9O molecules that are of almost identical energy (see above). While the Raman line observed at 425 cm^{-1} matches a calculated frequency of *exo*-S_9O, the signals observed at 350 and 314 cm^{-1} are in agreement with the data of *endo*-S_9O only. The six lines in the S–O stretching region also indicate two isomers together with additional factor group splittings. The agreement between calculated and measured wavenumbers is astonishingly good. Interestingly, the relative Raman intensities are quite different for the two conformers. In particular, the S–O stretching mode of *exo*-S_9O has

the highest Raman intensity, while it is only weak in *endo*-S_9O. The heterocyclic isomer **6c** can definitely be ruled out (see Table S4).

S_5O: The only experimental information on the vibrational spectra of S_5O is the S–O stretching frequency of the homocyclic compound dissolved in $CHCl_3$.[30] The recorded value of 1119 cm^{-1} is in agreement with a sulfoxide group attached to two sulfur atoms (Table 9).

Table 9. Calculated fundamental modes of homocyclic S_5O **2a**.[a]

Calcd wavenumber (Raman/IR intensity)	Assignment
1191 (92/100)	ν(SO)
517 (81/1)	ν(SS)
481 (26/4)	ν(SS)
419 (46/3)	ν(SS)
399 (45/13)	δ(SSO)
321 (100/5)	ν(SS) + δ(SSO)
302 (55/2)	ν(SS) + δ(SSO)
274 (47/0)	δ(SSS)
250 (43/0)	δ(SSS) + τ
223 (54/0)	ν(SS) + δ(SSO) + τ
201 (18/1)	τ + δ(SSO)
71 (10/1)	τ

[a] Wavenumbers in cm^{-1} and relative Raman/IR intensities in parentheses. For symbols and abbreviations, see Table 5.

Table 10. Calculated fundamental modes and IR intensities of the S_4O isomers **1a** and **1c**.[a]

Calcd wavenumber of **1a** (rel. Raman/IR intensity)	Assignment of **1a**	Calcd wavenumber of **1c** (rel. Raman/IR intensity)	Assignment of **1c**
1180 (29/100), a	ν(SO)	1230 (59/100), a′	ν(SO)
661 (41/70), a	ν(SS)	517 (100/5), a′	ν(SS)
490 (100/26), a	ν(SS)	454 (20/8), a″	ν(SS)
366 (28/8), a	ν(SS)	425 (12/13), a′	ν(SS) + δ(SSO)
308 (26/3), a	δ(SSS) + τ	394 (31/5), a″	ν(SS)
286 (34/3), a	δ(SSO)	308 (52/3), a′	δ(SSO) + δ(SSS)
223 (59/1), a	δ(SSS)	266 (34/0), a′	δ(SSS)
184 (38/1), a	δ(SSS) + τ	186 (32/0), a″	δ(SSO) + ν(SS)
111(18/0), a	δ(SSS) + τ	112 (3/0), a′	τ + δ(SSS)

[a] Wavenumbers in cm^{-1} and relative Raman/IR intensities in parentheses. For symbols and abbreviations, see Table 5.

S_4O: No experimental data whatsoever are available for S_4O. The calculated frequencies of the isomers **1a** and **1c** are compiled in Table 10. These data allow the identification of S_4O and its conformation once the compound has been prepared.

Vibrations of the heterocyclic isomers of the oxides S_4O to S_9O: The fundamental modes of the heterocyclic isomers S_nO are listed in Table S4. Most interesting are the two S–O stretching modes, which are calculated to occur in the region 574–649 cm^{-1} and which generally are of high IR intensity. On the other hand, the totally symmetrical ring bending ("breathing") vibration is of high Raman intensity and can be used to identify these species. The wavenumber of this mode depends on the ring size as the following data demonstrate (in cm^{-1}): S_4O (**1e**): 418; S_5O (**2d**): 322; S_6O (**3c**): 293; S_7O (**4c**): 209; S_8O (**5c**): 194; S_9O (**6c**): 160.

Conclusion

We have shown that the structures and/or vibrational spectra of S_6O, S_7O, S_8O, and S_9O are reproduced well by calculations according to G3X(MP2) theory. Therefore, reliable predictions can be made regarding other monoxides of sulfur, such as S_4O and S_5O, the most stable isomers of which are also homocyclic. Numerous other isomers of the S_nO molecules with $n = 4$–9 have been identified on the potential energy surfaces of the corresponding composition. The homolytic ring-opening energy increases with the ring size. Heterocyclic unbranched species are 17–54 kJ mol^{-1} less stable than the global minimum structures. The main discovery made in this work is the seemingly omnipresent π^*–π^* bonding interaction that determines the structures and conformations of all sulfur-rich binary oxides. It can be identified in all *cis*-planar (or almost planar) structural units of the types S=S-S=O and S=S-S=S where the sign "=" denotes a much shorter bond than the corresponding single bonds "S–S" or "S–O". This special interaction is responsible for the large number of isomers in addition to the expected homocyclic rings and unbranched chains. Another consequence is the wide variation of the S–S bond lengths, which range from 191.9 to 243.0 pm in the most stable molecules investigated.

All lower sulfur oxides decompose thermally to SO_2 and elemental sulfur (S_8). The related absolute reaction enthalpies are predicted to decrease with increasing S:O ratio from -345.5 kJ mol^{-1} (S_4O) to -209.0 kJ mol^{-1} (S_8O) if all reactants are gaseous. This trend is in agreement with the increasing thermal stability if the oxygen content decreases. While solid S_8O and S_9O can be kept at room temperature for several hours without decomposition, S_7O and S_6O decompose at 20 °C within 120 minutes, S_5O is known only in cold dilute solutions, and S_4O has not yet been prepared.

Acknowledgements

This work was supported by the National University of Singapore and the Norddeutscher Verbund für Hoch- und Höchstleistungsrechnen.

[1] For reviews, see: a) *Gmelin Handbuch der Anorganischen Chemie*, 8th ed., Schwefel, Ergänzungsband 3, Springer, Berlin, **1980**; b) R. Steudel, *Comments Inorg. Chem.* **1982**, *1*, 313–327; c) R. Steudel, *Phosphorus Sulfur Relat. Elem.* **1985**, *23*, 33–64; d) R. Steudel, *Top. Curr. Chem.* **2003**, *231*, 203–230.

[2] The most recent members added to this group are S_2O_3 and S_3O, detected by MS-MS techniques: F. Cacace, R. Cipollini, G. de Petris, M. Rosi, A. Troiani, *J. Am. Chem. Soc.* **2001**, *123*, 478–484; F.

Cacace, G. de Petris, M. Rosi, A. Troiani, *Chem. Commun.* **2001**, 2086–2087.
[3] R. Steudel, T. Sandow, *Inorg. Synth.* **1982**, *21*, 172.
[4] R. Steudel, J. Steidel, *Angew. Chem.* **1978**, *90*, 134–135; *Angew. Chem. Int. Ed. Engl.* **1978**, *17*, 134–135; J. Steidel, *Doctoral Dissertation*, Technical University of Berlin, **1983**.
[5] R. Steudel, T. Sandow, *Angew. Chem.* **1976**, *88*, 854–855; *Angew. Chem. Int. Ed. Engl.* **1976**, *15*, 772–773, and unpublished results.
[6] R. Steudel, T. Sandow, *Angew. Chem.* **1978**, *90*, 644–645; *Angew. Chem. Int. Ed. Engl.* **1978**, *17*, 612–613.
[7] R. Steudel, M. Rebsch, *Angew. Chem.* **1972**, *84*, 344–345; *Angew. Chem. Int. Ed. Engl.* **1972**, *11*, 302–303; R. Steudel, J. Latte, *Angew. Chem.* **1974**, *86*, 648–649; *Angew. Chem. Int. Ed. Engl.* **1974**, *13*, 603–604; R. Steudel, M. Rebsch, *Z. Anorg. Allg. Chem.* **1975**, *413*, 252–260.
[8] R. Steudel, T. Sandow, J. Steidel, *Z. Naturforsch. B* **1985**, *40*, 594–600.
[9] R. Steudel, R. Reinhardt, T. Sandow, *Angew. Chem.* **1977**, *89*, 757–758; *Angew. Chem. Int. Ed. Engl.* **1977**, *16*, 716–717.
[10] R. Reinhardt, *Doctoral Dissertation*, Free University of Berlin, **1978**. According to this thesis, the geometrical parameters of S_7O given in reference [9] are partly in error. The correct data are cited in reference [1a].
[11] R. Steudel, P. Luger, H. Bradaczek, M. Rebsch, *Angew. Chem.* **1973**, *85*, 452–453; *Angew. Chem. Int. Ed. Engl.* **1973**, *12*, 423–424; P. Luger, H. Bradaczek, R. Steudel, M. Rebsch, *Chem. Ber.* **1976**, *109*, 180–184.
[12] D. Hohl, R. O. Jones, R. Car, M. Parrinello, *J. Am. Chem. Soc.* **1989**, *111*, 825–828.
[13] R. O. Jones, *Inorg. Chem.* **1994**, *33*, 1340–1343.
[14] M. W. Wong, R. Steudel, *Chem. Commun.* **2005**, 3712–3714.
[15] R. Steudel, Y. Steudel, *Eur. J. Inorg. Chem.* **2004**, 3513–3521.
[16] a) Y. Drozdova, R. Steudel, *Chem. Eur. J.* **1995**, *1*, 193- 198; b) A. Shaver, M. El-khateeb, A.-M. Lebuis, *Angew. Chem.* **1996**, *108*, 2510–2512; *Angew. Chem. Int. Ed.* **1996**, *35*, 550–552.
[17] W. Nehb, K. Vydra, in *Ullmann's Encyclopedia of Industrial Chemistry, Vol. A25*, VCH, Weinheim, **1994**, p. 507–567.
[18] *Ullmann's Encyclopedia of Industrial Chemistry, Vol. A25*, VCH, Weinheim, **1991**, p. 73–124.
[19] Kirk-Othmer *Encyclopedia of Chemical Technology, 4th* ed., *Vol. 18*, **1996**, p. 433–469.
[20] L. A. Curtiss, P. C. Redfern, K. Raghavachari, J. A. Pople, *J. Chem. Phys.* **2001**, *114*, 108–117.
[21] L. A. Curtiss, P. C. Redfern, K. Raghavachari, V. Rassolov, J. A. Pople, *J. Chem. Phys.* **1999**, *110*, 4703–4709.
[22] R. O. Roos, *Adv. Chem. Phys.* **1987**, *69*, 399.
[23] H.-J. Werner, *Mol. Phys.* **1996**, *89*, 645–661.
[24] H.-J. Werner, P. Knowles, *J. Chem. Phys.* **1988**, *89*, 5803–5814.
[25] A. E. Reed, L. A. Curtiss, F. Weinhold, F. *Chem. Rev.* **1988**, *88*, 899–926.
[26] M. Messerschmidt, A. Wagner, M. W. Wong, P. Luger, *J. Am. Chem. Soc.* **2002**, *124*, 732–733.
[27] R. F. W. Bader, *Atoms in Molecules - A Quantum Theory*, Oxford University Press, Oxford, **1990**.
[28] GAUSSIAN 98, M. J. Frisch, G. W. Trucks, H. B. Schlegel, G. E. Scuseria, M. A. Robb, J. R. Cheeseman, V. G. Zakrzewski, J. A. Montgomery, Jr., R. E. Stratmann, J. C. Burant, S. Dapprich, J. M. Millam, A. D. Daniels, K. N. Kudin, M. C. Strain, O. Farkas, J. Tomasi, V. Barone, M. Cossi, R. Cammi, B. Mennucci, C. Pomelli, C. Adamo, S. Clifford, J. Ochterski, G. A. Petersson, P. Y. Ayala, Q. Cui, K. Morokuma, D. K. Malick, A. D. Rabuck, K. Raghavachari, J. B. Foresman, J. Cioslowski, J. V. Ortiz, A. G. Baboul, B. B. Stefanov, G. Liu, A. Liashenko, P. Piskorz, I. Komaromi, R. Gomperts, R. L. Martin, D. J. Fox, T. Keith, M. A. Al-Laham, C. Y. Peng, A. Nanayakkara, C. Gonzalez, M. Challacombe, P. M. W. Gill, B. Johnson, W. Chen, M. W. Wong, J. L. Andres, C. Gonzalez, M. Head-Gordon, E. S. Replogle, J. A. Pople, Gaussian Inc., Pittsburgh, PA, **1998**.
[29] MOLPRO, version 2002, H.-J. Werner, P. J. Knowles, M. Schütz, R. Lindh, P. Celani, T. Korona, G. Rauhut, F. R. Manby, R. D. Amos, A. Bernhardsson, A. Berning, D. L. Cooper, M. J. O. Deegan, A. J. Dobbyn, F. Eckert, C. Hampel, G. Hetzer, A. W. Lloyd, S. J. McNicholas, W. Meyer, M. E. Mura, A. Nicklaß, P. Palmieri, R. Pitzer, U. Schumann, H. Stoll, A. J. Stone R. Tarroni, T. Thorsteinsson, University of Birmingham, **2002**.
[30] W. Genz, P. W. Schenk, *Z. Anorg. Allg. Chem.* **1970**, *379*, 300; W. Genz, *Doctoral Dissertation*, Technical University of Berlin, **1969**.
[31] M. W. Wong, R. Steudel, *Phys. Chem. Chem. Phys.* **2006**, *8*, 1291–1297.
[32] a) V. Jonas, G. Frenking, *Chem. Phys. Lett.* **1991**, *177*, 175–183; b) A. Timoshkin, G. Frenking, *J. Chem. Phys.* **2000**, *113*, 8430–8433.
[33] M. W. Wong, Y. Steudel, R. Steudel, *J. Chem. Phys.* **2004**, *121*, 5899–5907.
[34] M. W. Wong, Y. Steudel, R. Steudel, *Inorg. Chem.* **2005**, *44*, 8908–8915.
[35] D. D. Gregory, W. S. Jenks, *J. Phys. Chem. A* **2003**, *107*, 3414–3423.
[36] M. W. Wong, R. Steudel, *Chem. Phys. Lett.* **2003**, *379*, 162–169.
[37] A. Z. Rys, A.-M. Lebuis, A. Shaver, D. N. Harpp, *Organometallics* **1999**, *18*, 1113–1115.
[38] R. Steudel, J. Steidel, J. Pickardt, *Angew. Chem.* **1980**, *92*, 313–314; *Angew. Chem. Int. Ed. Engl.* **1980**, *19*, 325–326.
[39] A. Ishii, H. Oshida, J. Nakayama, *Bull. Chem. Soc. Japan* **2002**, *75*, 319–328.
[40] R. Steudel, J. Steidel, J. Pickardt, F. Schuster, R. Reinhardt, *Z. Naturforsch. B* **1980**, *35*, 1378–1383.
[41] R. Steudel, F. Schuster, *J. Mol. Struct.* **1978**, *44*, 143–157.
[42] R. Steudel, A. Prenzel, J. Pickardt, *Angew. Chem.* **1991**, *103*, 586–588, *Angew. Chem. Int. Ed. Engl.* **1991**, *30*, 550–552.
[43] R. Steudel, *Angew. Chem.* **1975**, *87*, 683–692; *Angew. Chem. Int. Ed. Engl.* **1975**, *14*, 655–664.
[44] A. Bondi, *J. Phys. Chem.* **1964**, *68*, 441–451.
[45] M. W. Wong, Y. Steudel, R. Steudel, *Chem. Phys. Lett.* **2002**, *364*, 387–392.
[46] H.-J. Hecht, R. Reinhardt, R. Steudel, H. Bradaczek, *Z. Anorg. Allg. Chem.* **1976**, *426*, 43–48.
[47] R. Steudel, T. Sandow, J. Steidel, *J. Chem. Soc. Chem. Commun.* **1980**, 180–181.
[48] R. Steudel, K. Bergemann, J. Buschmann, P. Luger, *Inorg. Chem.* **1996**, *35*, 2184–2188.
[49] The motif is defined as the order of signs of the S-S-S-S torsion angles around the ring.
[50] R. Steudel, J. Steidel, R. Reinhardt, *Z. Naturforsch. B* **1983**, *38*, 1548–1556; R. Reinhardt, R. Steudel, F. Schuster, *Angew. Chem.* **1978**, *90*, 55–56; *Angew. Chem. Int. Ed. Engl.* **1978**, *17*, 57–58.
[51] R. Steudel, *Z. Naturforsch. B* **1975**, *30*, 281–282.
[52] R. Steudel, M. Rebsch, *J. Mol. Spectrosc.* **1974**, *51*, 334–340.
[53] R. Steudel, D. F. Eggers, *Spectrochim. Acta* **1975**, *31A*, 871–877.

Received: March 20, 2006
Revised: May 12, 2006
Published online: October 2, 2006

